PAPER

Yielding and resolidification of colloidal gels under constant stress

IOP Publishing Journal of Physics: Condensed Matter
J. Phys.: Condens. Matter **33** (2021) 284002 (12pp) https://doi.org/10.1088/1361-648X/abfb8d

Yielding and resolidification of colloidal gels under constant stress

Esmaeel Moghimi[1], Andrew B Schofield[2] and George Petekidis[1,*]

[1] FORTH/IESL and Department of Materials Science and Technology, University of Crete, 71110 Heraklion, Greece
[2] School of Physics and Astronomy, The University of Edinburgh, EH9 3FD, Scotland, United Kingdom

E-mail: georgp@iesl.forth.gr

Received 19 January 2021, revised 9 April 2021
Accepted for publication 26 April 2021
Published 3 June 2021

Abstract

We examine the macroscopic deformation of a colloidal depletion gel subjected to a step shear stress. Three regimes are identified depending on the magnitude of the applied stress: (i) for stresses below yield stress, the gel undergoes a weak creep in which the bulk deformation grows sublinearly with time similar to crystalline and amorphous solids. For stresses above yield stress, when the bulk deformation exceeds approximately the attraction range, the sublinear increase of deformation turns into a superlinear growth which signals the onset of non-linear rearrangements and yielding of the gel. However, the long-time creep after such superlinear growth shows two distinct behaviors: (ii) under strong stresses, a viscous flow is reached in which the strain increases linearly with time. This indicates a complete yielding and flow of the gel. In stark contrast, (iii) for weak stresses, the gel after yielding starts to resolidify. More homogenous gels that are produced through enhancement of either interparticle attraction strength or strain amplitude of the oscillatory preshear, resolidify gradually. In contrast, in gels that are more heterogeneous resolidification occurs abruptly. We also find that heterogenous gels produced by oscillatory preshear at intermediate strain amplitude yield in a two-step process. Finally, the characteristic time for the onset of delayed yielding is found to follow a two-step decrease with increasing stress. This is comprised of an exponential decrease at low stresses, during which bond reformation is decisive and resolidification is detected, and a power law decrease at higher stresses where bond breaking and particle rearrangements dominate.

Keywords: colloidal gels, yielding, creep, resolidification

Supplementary material for this article is available online

(Some figures may appear in colour only in the online journal)

1. Introduction

Attractive colloidal systems are ubiquitous in nature as well is in industrial systems and daily life products such as foodstuff, personal care products or even slurries such as construction materials like cement [1]. Therefore, their rheological behavior is relevant to a wide range of applications and products particularly in their processing, transportation and shelf-life. A common phenomenon in such multicomponent complex soft matter formulations is the interplay between the attractive and repulsive interactions, thermal Brownian motion and external fields such as gravity or flow [1].

When attractive interactions dominate colloidal particles form clusters that, depending on the particle volume fraction and attraction strength, may create interconnecting networks and gels with solid like mechanical response with a finite yield stress that needs to be exceeded to induce flow in the system. The underlying structure responsible for the solid like

* Author to whom any correspondence should be addressed.

response range from dilute fractal-like networks of thin strands [1, 2], concentrated interconnected glassy clusters formed via arrested phase separation [3–6] to more homogeneous cages in attractive glasses at very high volume fractions [7, 8].

Yield stress systems composed of attractive particles often exhibit ageing, as their mechanical properties, internal dynamics and microstructure are changing with time [9]. On the other hand shear and flow affect the formation or breakage of clusters and gel network commonly seen also in industrial formulations. Hence, such interplay of structural evolution and flow properties introduce a shear-history dependence, commonly termed as thixotropy [1, 10, 11]. For example in transient tests such as a start-up shear rate or a start-up shear stress the stress or acquired strain, respectively, depend on the ageing time of the sample [12–14]. Similar behavior has been observed in step-up or step-down shear rate or shear reversal tests. Therefore, the linear and nonlinear rheological response of gels depend on the time after their formation or after shear rejuvenation. The latter, a procedure that aims to eliminate history effects and reset the internal time of the sample, consists of some type of strong, steady or oscillatory shearing that involves high stresses and shear rates [9, 15–17]. Moreover in such systems gravity can also play a role in causing gel collapse, effectively limiting the lowest volume fraction the gel can be stable [18, 19] while other effects that might be present are wall slip and shear banding [20–22].

On the microstructural level arrested phase separation gels exhibit coarsening, especially when the attraction strength is not much larger than the thermal energy so that thermal fluctuations may induce bond restructuring within the clusters. If, however, the attraction strength is several k_BT, coarsening becomes extremely slow and structure, dynamics and mechanical properties are essentially frozen [23, 24].

Whereas colloidal gels yield by the application of any finite constant shear rate, under the application of constant stress yielding is achieved only at stresses above the yield stress while at lower values the strain is expected to slowly creep towards a constant plateau value. In practice colloidal gels exhibit a long transient creep response for stresses around the yield stress due to their heterogeneous structure which is amenable to large-scale, stress induced restructuring. This has been manifested in the transient response by phenomena such as delayed yielding and delayed solidification taking place before a final steady state is reached [25–27]. In the former case a colloidal gel under constant stress eventually yields and flows with a constant viscosity after a transient period during which it exhibits an apparent solid like response. The latter is composed of an initial elastic response at early times and a subsequent slow creep with nonlinear deformation at intermediate but often prolonged time period. This response has been seen in several experimental systems and is related either with a catastrophic failure of the gel structure or to more subtle bond breaking that enables larger level particle rearrangements, leading in both cases to flow after a delay time, which decreases with applied stress [27–29]. On the other hand, colloidal gels have been proposed to exhibit a delayed solidification under constant stress, during which a sample that initially seems to flow, subsequently re-solidifies again due to shear induced structural changes. Such behavior has been found in computer simulations for particles with moderate attractions of few k_BT, where depending on the applied stress three characteristic responses were detected [25]. For stresses well above the yield stress yielding leads to steady state flow with a constant shear rate while well below the yield stress the sample slowly creep with a progressively decreasing shear rate. Near the yield stress however the gel may respond in a more complex way exhibiting a delayed solidification after it has temporarily yielded and been flowing. These phenomena demonstrate the complex interplay of stress induced restructuring, involving restructuring and breakage of bonds with bond reformation that trigger cluster and network reformation or disintegration.

A common phenomenology in a wide range of yield stress fluids for stresses below the yield stress is a sublinear decay of the shear rate with time, following an Andrade type decay proportional to $t^{-2/3}$. Although the details of the underlying structural mechanism might be different in soft matter systems such as colloidal gels [29], repulsive glasses of hard [30] or soft particles [31], the general perception is that it is related to the similar phenomena of the collective propagation of local dislocations in metallic solids.

Delayed yielding has been quantified by the measurement of the characteristic time linked with the onset of flow after stress is applied. This delay time, τ_d, is a decreasing function of the applied stress as has been seen in a variety of systems [27, 28, 32] to follow a two-step decay with the delay time decreasing exponentially in both regimes. This behavior was attributed to a bond rupture model that led to macroscopic gel failure and flow [27, 28], or in another study involving carbon black particle gels, it was related to distinct transitions from localized flow (wall slip) to homogenous flow conditions [29].

While delayed yielding has been seen experimentally in a variety of systems such as carbon black, depletion gels, thermoreversible gels [27, 33], or even protein gels [34, 35], the delayed resolidification found in simulations [25] has not been detected in real experimental systems so far. Here we present a systematic study in intermediate volume fraction, depletion gels of polymethyl-methacrylate (PMMA) particles at different attraction strengths, where we follow the transient response of the system at applied shear stress below and above the yield stress. Moreover, the effect of preshear and ageing time before the application of stress was also probed in an order to investigate how preshear history affects the creep response. Our experimental findings show that both delayed yielding and delayed solidification is detected with the response depending both on the attraction strength and pre-shear conditions.

The rest of the paper is organized as follows: we first present the experimental system and the rheological protocols in the materials and methods section. We then present the results of creep data as a function of shear stress for strong and subsequently for lower attraction strengths. We then discuss creep response at different pre-shear histories where we vary both the pre-shear conditions and the ageing time, and finally present a discussion and conclusions.

2. Materials and Methods

We used nearly hard-sphere colloidal particles made of PMMA. Particles are sterically stabilized by a short grafted layer ($\sim$10 nm) of poly-hydroxystearic acid chains. Particles have a hydrodynamic radius of $R_h = 196$ nm with the polydispersity of about 12% (determined by light scattering) to suppress crystallization. They were dispersed in octadecene which has a high boiling point (315 °C) that minimizes evaporation and allows for long-time rheological experiments. The depletion attractions were introduced between particles by adding non-adsorbing linear 1,4-polybutadiene chains with molecular weight, $M_w = 323\,300$ g mol^{-1} and radius of gyration, $R_g = 19$ nm (measured by light scattering). This gives a polymer-colloid size ratio $\xi = R_g/R = 0.097$ in dilute solution. The gel was prepared at particle volume fraction $\phi = 0.3$ and two different polymer concentrations of $c_p/c_p^* = 0.186$ and 0.589, where c_p^* $(= 3M_w/(4\pi N_A R_g^3) = 0.0187$ g cm^{-3} with N_A being Avogadro's number) is the polymer overlap concentration. The attractive potential was estimated by generalized free volume theory (GFVT) [36] which provides a better approximation compared to original Asakura–Oosawa model [37]. Theory predicts the polymer concentration in the free volume accessible for polymers as $c_p^{free}/c_p^* = 0.303$, and 0.913, respectively. According to GFVT, the effective polymer-colloid size ratio reduces to $\xi^* = 0.09$, and 0.058 and the corresponding attraction strengths at contact are $U_{dep}(2R) = -5.7$ and $-12.7k_BT$, respectively.

Rheological experiments were performed with Anton-Paar MCR 501 rheometer. Serrated homemade cone-plate geometries with diameter 25 mm, cone angle 2.3° and cone truncation 0.05 mm were used. Adopting such roughened geometries suppresses wall-slip. This is evidenced by the absence of the second pseudo-yield stress plateau at low shear rates in the flow curve (see figure 9) which is the rheological signature of the wall-slip [20]. Measurements were conducted at $T = 20$ °C using a Peltier plate.

2.1. Shear rejuvenation protocol

In order to erase any history effects, before each experiment, first the gel was subjected to a large amplitude oscillatory shear (LAOS) flow with the strain amplitude of $\gamma_0 = 1000\%$ and frequency $\omega = 10$ rad s^{-1}. In order to examine if the imposed shear flow is strong enough to fully break the bonds between the particles, we use Péclet depletion number (the ratio of shear forces F_{shear} to attractive forces due to depletion interactions F_{dep}) [17, 38, 39]:

$$Pe_{dep} = \frac{F_{shear}}{F_{dep}} = \frac{12\pi\eta\xi R^3}{U_{dep}(2R)}\gamma_0\omega. \quad (1)$$

A shear rejuvenation protocol demands $Pe_{dep} > 1$ which means a stronger shear forces compared to attractive forces and hence a substantial number of bonds are expected to break under shear. For the shear rejuvenation used in this study i.e. $\gamma_0 = 1000\%$ and $\omega = 10$ rad s^{-1}, the vales of Pe_{dep} for the gels with -5.7 and $-12.7k_BT$ are $Pe_{dep} = 5$ and 2.2, respectively. Hence, the imposed shear flow is sufficient to break-down the gel structure, allowing for a dispersed configuration. After shear rejuvenation, flow is stopped and the gel is allowed to age for a certain duration of time before it is subjected to a step-stress.

In order to investigate the effect of the shear history on the yielding of the gel during creep measurements, first the gel was shear rejuvenated with $\gamma_0 = 1000\%$ and $\omega = 10$ rad s^{-1}. Then, the gel was directly subjected to an oscillatory shear with the same frequency but with different strain amplitudes of $\gamma_0 = 100\%$ and 25%. After reaching a constant values of both elastic G' and viscous G'' moduli, the shear was stopped and the gel was allowed to age for the duration of 1000 s before the step-stress is applied.

In the present study, we compare our experimental results with those from BD simulations on lower volume fraction ($\phi = 0.2$) colloidal gels [25]. We must note that the initial condition in our experiments and simulations are different. As mentioned above, in experiments the gel is shear rejuvenated by LAOS flow with $Pe_{dep} > 1$. In contrast, in BD simulations the gel has been prepared by switching on the attractions from an already equilibrated suspension of purely repulsive particles. A direct comparison between rheo-confocal experiments and BD simulations demonstrates that high preshear (for $Pe_{dep} > 1$) and thermal quench are expected to produce similar relatively homogenous structures [16]. Hence, our creep data for those gels presheared at large strain amplitudes can be contrasted with those from simulations. On the other hand, a low/intermediate strain amplitude preshear will create highly heterogeneous structures [17] and hence its comparison with simulations is subjected to uncertainty.

3. Results and discussion

3.1. Creep experiments

In creep measurements, the sample is subjected to a constant shear stress and the evolution of the strain, $\gamma(t)$, with time is probed and the creep compliance, the ratio of time-dependent strain to the applied stress, $J(t) = \gamma(t)/\sigma$ is calculated. The generalized Stokes–Einstein relation (GSER) reveals that the macroscopic deformation $J(t)$ is linearly linked to the microscopic average mean-squared displacements of the probed colloidal particles embedded in the fluid [40–43]:

$$J(t)k_BT/(\pi R^3) = \langle \Delta r^2 \rangle / R^2. \quad (2)$$

Although the validity of GSER and the extent of the agreement between macro and microrheology may be limited for some systems and conditions [40, 44], we cautiously use it here to allow discussion of creep response in analogy to the particle dynamics. Moreover, as mentioned, the relation in equation (2) links $J(t)$ measured in creep experiments to the MSD of a probe particle in the quiescent sample. However, the work of Sentjarbrckaja *et al* [13] has shown that even at the nonlinear shear for systems out of equilibrium, $J(t)$ and MSD exhibit an analogous response, being proportional to the macroscopic strain deformation. Here, we exploit qualitatively such analogy to interrogate the response of colloidal gels under constant stress.

Note also that recent combined simulation and rheometry studies in colloidal gels [24], examining the level of GSER validity with respect to link between linear viscoelasticity and average particle dynamics has showed that the latter may represent only approximately the macroscopic linear viscoelasticity only for rather strong homogenous gels.

In this section, we examine the response of an intermediate volume fraction ($\phi = 0.3$) colloidal gel to a step shear stress. A wide range of shear stresses varying from below to well above the yield stress is investigated while the deformation of the gel over time is probed. We additionally examine the effect of gel age, interparticle attraction strength as well as preshear history on the yielding behavior of the gel during creep measurements. We first discuss the creep results for the gel with the stronger attraction strength of $U_{\text{dep}}(2R) = -12.7k_{\text{B}}T$. The gel has been shear rejuvenated at the strain amplitude of $\gamma_0 = 1000\%$ with $\omega = 10$ rad s^{-1} and aged afterwards for the duration of 1000 s before it is subjected to a step stress. The results of creep experiments are shown in figure 1. Here, the creep compliance is presented in the form of $J(t)k_{\text{B}}T/(\pi R^3)$. As mentioned above, such normalization allow us to make a link between macroscopic deformation and microscopic particle dynamics during creep measurements (see equation (2)). Moreover the time is normalized by Brownian time in the dilute regime as $t_{\text{B}} = 6\pi\eta R^3/k_{\text{B}}T = 0.15$ where $\eta = 4.2$ mPa is the solvent viscosity, k_{B} is Boltzmann's constant and T is the temperature. We must note that the Brownian time in dilute regime is the simplest scaling to be considered. In the concentrated glassy clusters, hydrodynamic interactions are expected to increase the Brownian relaxation time by about an order of magnitude akin to HS glasses [45]. Moreover, the presence of a polymer depletant (through an increase of the background viscosity) and attractions are also additional factors that slow down the short-time self-diffusivity. However, for the simplicity reasons, we have not taken these effects into account here.

For all shear stresses examined here, the creep compliance exhibits an initial fast growth for $t/t_{\text{B}} < 1$ which is stress independent. This initial growth is followed by the resonant 'creep ringing' which originates from an interplay of the motor inertia with the gel elasticity [46]. Here, the short-time ($t/t_{\text{B}} < 1$) creep deformation scales with the square of time ($J(t) \sim t^2$). However, this initial superlinear increase of $J(t)$ is due to rheometere's inertia rather than a true response of the gel. Brownian dynamics (BD) simulations on the lower volume fraction colloidal gels ($\phi = 0.2$) show that the short-time bulk deformation scales with the square root of time ($J(t) \sim t^{0.5}$) regardless of gel age or bond strength [25]. This short-time deformation corresponds to the high-frequency linear viscoelastic response, where only some structural deformation takes place.

For $\sigma < 0.7$ Pa, the creep compliance is independent of the stress throughout the creep measurement. Hence, here we define the yield stress as the stress below which creep compliance becomes stress-independent. For times beyond creep ringing ($t/t_{\text{B}} > 1$) and for $\sigma < \sigma_y$, $J(t)$ shows a plateau which is followed by a weak sublinear increase at longer times. Based on equation (2), this plateau represents the length scale at which particles are localized due to short-ranged interparticle attractions. The plateau (or localization length) is slightly smaller than the attraction range in agreement with findings from BD simulations that show particles are localized at length scales smaller that the range of attraction [24, 39, 47, 48].

The long-time pre-yield response of the gel is better seen by plotting the shear rate, $\dot{\gamma}(t) = \mathrm{d}\gamma/\mathrm{d}t$, the time derivative of the bulk deformation (figure 1(b)). Similar to $J(t)$, here we present the shear rate in the form of $\dot{\gamma}(t)k_{\text{B}}T/(\sigma\pi R^3)$ (figure 1(b)). Based on equation (2), $\dot{\gamma}(t)k_{\text{B}}T/(\sigma\pi R^3)$ represents an instantaneous diffusivity ($D = \mathrm{d}(\langle\Delta r^2\rangle/R^2)/\mathrm{d}t$). Moreover, this ratio is equivalent to the inverse instantaneous viscosity ($k_{\text{B}}T/(\eta\pi R^3)$). For $\sigma < 0.7$ Pa and $t/t_{\text{B}} > 10$ (above the resonant 'creep ringing'), the shear rate decays continuously with time. The decay follows two distinct patterns: (i) at intermediate times ($1 < t/t_{\text{B}} < 1000$), the shear rate follows a power law decay with $\dot{\gamma} \propto t^{-2/3}$. Such power law decay of shear rate has been observed first in metals and it is known as Andrade creep [49] also known as β creep. It has been found also in gels and colloidal glasses [31, 50]. (ii) At even longer times, the creep response seems to follow a linear decrease with time ($\dot{\gamma} \propto t^{-1}$). This has first been introduced by Phillips (also called α creep) in hard matter [51] and was also reported for granular systems and colloidal glasses [31, 52]. Such algebraic decay of shear rate indicates that the gel undergoes plastic deformations under weak stresses rather than recoverable linear viscoelastic extension [25]. The algebraic decay of shear rate originates from thermal fluctuations. In the absence of Brownian motions, the gel behaves as a linear elastic solid in which the shear rate decays exponentially over time [25]. Microstructural analysis from BD simulations for $\sigma < \sigma_y$ indicates a net bond formation and hence gel coarsening under such weak stresses [25].

When shear stress is increased above σ_y, at short times $J(t)$ follows the curves for $\sigma < \sigma_y$. However, after a certain time, $J(t)$ deviates from the ones for $\sigma < \sigma_y$ and crosses over to values higher than the attraction range. As stress is increased, this deviation takes place at shorter times. In this regime, $J(t)$ exhibits a superlinear increase with time where for $\sigma > 1$ Pa, it shows a ballistic growth i.e. $J(t) \sim t^2$ which consequently leads to a linear increase of $\dot{\gamma}$ with time (see figure 1(b)). Such ballistic growth of bulk deformation, based on equation (2), may originate from ballistic displacements of particles (i.e. $\langle\Delta r^2\rangle \sim t^2$) when they are subjected to $\sigma > \sigma_y$ as has been observed in hard-sphere colloidal glasses during creep measurements for $\sigma > \sigma_y$ [13]. In the case of *attractive colloidal glasses* during start-up shear flow, yielding commences by ballistic displacements of particles when they escape their attractive bonds [47]. Hence, one may expect a similar mechanism for colloidal gels as well where yielding during a step stress measurement may initiate through ballistic displacements of particles when they leave their local constrains caused by inter-particle attractions. As mentioned, this is manifested by the ballistic increase of $J(t)$ when deformations exceed the attraction range. Moreover, note that BD simulations on colloidal gels has shown a net, although limited, bond loss during the superlinear growth of $J(t)$ [25] in agreement with similar

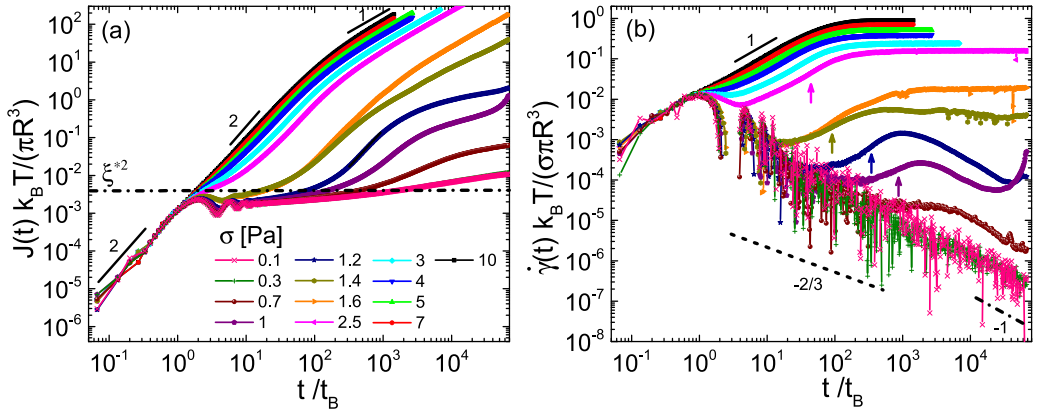

Figure 1. (a) Creep compliance and (b) the shear rate as a function of time at different applied shear stresses as shown in the legend. The horizontal dashed–dotted line in (a) marks ξ^{*2}. Dashed line in (b) represents Andrade creep law, $\dot{\gamma}(t) \propto t^{-2/3}$ and dashed–dotted line shows logarithmic creep, $\dot{\gamma}(t) \propto 1/t$. The vertical arrows in (b) show the delay yield time. Results are for the gel with $\phi = 0.3$, $U_{\rm dep}(2R) = -12.7k_{\rm B}T$ and $\xi^* = 0.058$. The gel has been shear rejuvenated with $\gamma_0 = 1000\%$ and $\omega = 10$ rad s^{-1} and aged for the duration of 1000 s before the stress is applied.

findings in experiments and BD simulation under constant shear rate [16, 53].

After the ballistic increase of the creep compliance and the initial yielding of the gel, two-distinct behaviors are detected: (i) For $\sigma > 1.4$ Pa, $J(t)$ exhibits a linear increase with time and consequently the shear rate reaches a constant value which indicates the development of a steady state viscous flow and hence a complete yielding. BD simulations has shown a significant net bond loss in this regime [25].

(ii) For an intermediate range of shear stresses (0.3 Pa $< \sigma <$ 1.6 Pa), however, an interesting response emerges where at long-times the gel starts to resolidify under stress. This is manifested by a transition in $J(t)$ from a superlinear to a sublinear growth and consequently a significant decrease of flow rate with time. As the imposed stress reduces, resolidification initiates at longer times and the reduction of flow rate is more intense in full agreement with findings from BD simulations [25]. Note that such resolidification during creep experiments has also been observed in concentrated suspensions of purely repulsive star polymers and been associated to the interplay between ageing and shear rejuvenation [26]. BD simulations for lower volume fraction colloidal gels $\phi = 0.2$ associates such macroscopic resolidification to a microscopic transition from a net bond loss, during the ballistic growth of $J(t)$, to a net bond formation during the resolidification process [25]. The resolidified gel is coarser compared to the quiescently aged gel. This is reminiscent of mechanisms under steady or oscillatory shear at low and intermediate shear rates or strain amplitudes that lead to cluster compactification [16, 17]. The examination of the delay yield time, as will be discussed later, and its dependence on shear stress provide insight into the microscopic origin of such resolidification under stress.

We should note that resolidification observed in our experiments might be transient. The gel after long-time resolidification may again start to yield and flow (for example see $\sigma = 1$ and 1.2 Pa in figure 1). This could originate from the partial collapse of the gel network. Note however that BD simulations which do not include density mismatch between particles and solvent and hence ignore any collapse of the gel network, also showed signatures of transient resolidification [25]. Therefore, it may not be excluded that under the appropriate conditions a system may exhibit continues transitions between successive yielding and resolidification.

As the final comment on this section, we point out that it would be interesting to examine the linear viscoelastic properties of the gel after log-time creep experiments to investigate whether the gel becomes weaker or stronger especially when it resolidifies under stress.

3.1.1. Effect of the gel age. In this section, we examine the effect of waiting time after shear rejuvenation or equivalently the gel age on the creep response. As the gel ages, its structure coarsens, more bonds are formed and as the result particle mobility is reduced and the gel elasticity is enhanced [16, 23, 24, 38].

In figure 1, we have discussed the creep response for the older gel of the same attraction strength $U_{\rm dep}(2R) = -12.7k_{\rm B}T$ which has been aged for the duration of 1000 s ($6667t/t_{\rm B}$) before the stress is applied. In figure 2, we present the creep response for the younger gel which has aged for 100 s after shear rejuvenation. The bulk deformation for the younger gel shows similar shear stress dependence as the one for the older gel: a creeping regime for $\sigma < 0.7$ Pa, a resolidification regime for 0.7 Pa $< \sigma <$ 1.8 Pa and a viscous flow regime for $\sigma > 1.6$ Pa. A careful comparison between old (figure 1) and young (figure 2) gels indicates that the older gel resolidifies faster over time compared to the younger gel. This may originate from an enhanced structural heterogeneity in the older gel. This idea will be further supported when the influence of bond strength (section 3.1.2) and preshear (section 3.1.3) are discussed.

In order to highlight the detailed differences between young and old gels during the creep measurements, we contrast the creep compliance and the shear rate for gels with two different ageing times of 100 s and 1000 s at three different regimes: (i) below the yield stress (ii) in the resolidification regime and (iii) viscous flow regime. Results of such comparison are shown

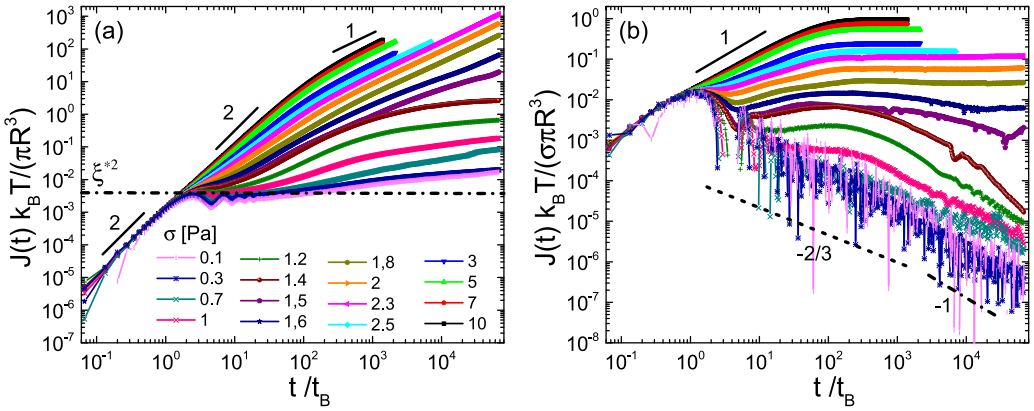

Figure 2. (a) Creep compliance and (b) the shear rate as a function of time at different applied shear stresses as shown in the legend. The horizontal dashed–dotted line in (a) marks $\xi*^2$. Dashed line in (b) represents Andrade creep law, $\dot{\gamma}(t) \propto t^{-2/3}$ and dashed–dotted line shows logarithmic creep, $\dot{\gamma}(t) \propto 1/t$. Results are for the gel with $\phi = 0.3$, $U_{\rm dep}(2R) = -12.7 k_{\rm B}T$ and $\xi^* = 0.058$. The gel has been shear rejuvenated with $\gamma_0 = 1000\%$ and $\omega = 10$ rad s^{-1} and aged for the duration of 100 s before the stress is applied.

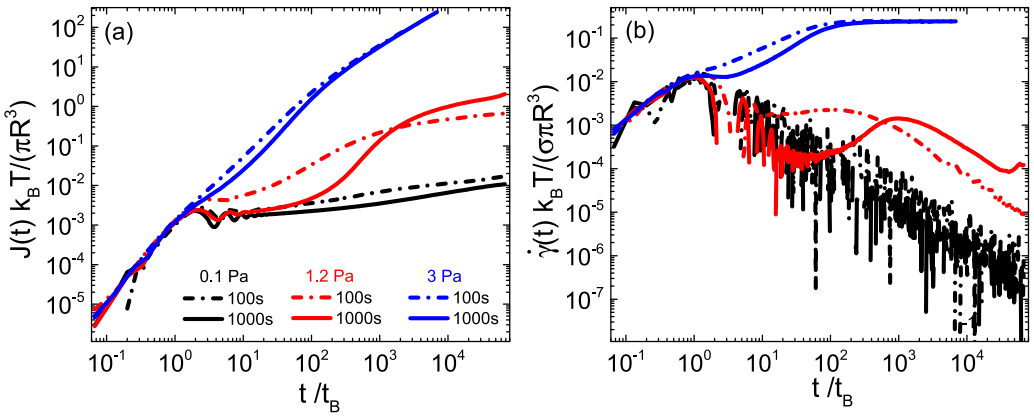

Figure 3. (a) Creep compliance and (b) the shear rate as a function of time at different applied shear stresses as shown in the legend for two different ageing times of 100 s (dashed–dotted lines) and 1000 s (solid lines). Results are for the gel with $\phi = 0.3$, $U_{\rm dep}(2R) = -12.7 k_{\rm B}T$ and $\xi^* = 0.058$. The gel has been shear rejuvenated with $\omega = 10$ rad s^{-1} and $\gamma_0 = 1000\%$.

in figure 3. For $\sigma < \sigma_y$, the older gel shows smaller values of creep compliance compared to the younger one. Based on equation (2), this indicates that in the older gel particles are less mobile and they are localized at smaller length scales consistent with previous observations [23, 24]. Moreover, lower values of $J(t)$ for the older gel means larger elasticity compared to younger gel since the complex modulus G^* is proportional to $1/J(t)$ [42]. This is in agreement with linear viscoelastic measurements which indicate that the gel gets stronger as it ages with elastic modulus G' increasing with time (see figure S1 (https://stacks.iop.org/JPCM/33/284002/mmedia)).

For $\sigma > \sigma_y$, the initial ballistic growth of $J(t)$ and hence yielding initiates at earlier times in the younger gel which has a higher particle mobility. This finding indicates that Brownian motion promotes yielding which is consistent with findings in gels during creep by BD simulations [25] as well as earlier experimental studies in similar depletion gels where the first yield strain related to bond rearrangements, was found to increase with frequency in LAOS experiments. The latter was attributed within a Kramer's escape model to effects of Brownian motion [54]. Note also that similar Brownian motion assisted yielding has been observed experimentally and by BD simulations in colloidal glasses where the yield strain both in oscillatory [55] and start-up shear [56] was found to decrease at lower frequencies or shear rates where Brownian motion dominates. Moreover, this idea that Brownian motions facilitates yielding will be further supported through the examination of interparticle attraction strength and range of attraction in section 3.1.2.

A different creep response is detected at long-times: in the viscous flow regime ($\sigma = 3$ Pa in figure 3), both young and old gels show identical long-time creep response. This indicates a unique shear-melted state where the structural history incorporated in the system during ageing has been completely erased by shear flow. In contrast, in the resolidification regime ($\sigma = 1.2$ Pa in figure 3), the long-time creep response for the young and old gels is different. The younger gel resolidifies earlier and the rate at which it resolidifies is more gradual compared to older gel; a finding that is in agreement with BD simulations [25].

3.1.2. Effect of the depletant concentration. In this section, we examine the influence of depletant concentration on the

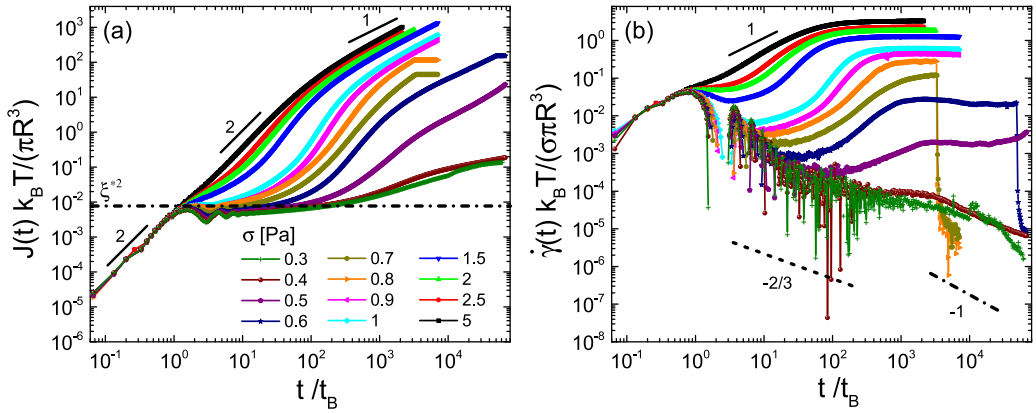

Figure 4. (a) Creep compliance and (b) the shear rate as a function of time at different applied shear stresses as shown in the legend. The horizontal dashed–dotted line in (a) marks $\xi*^2$. Dashed line in (b) represents Andrade creep law, $\dot{\gamma}(t) \propto t^{-2/3}$ and dashed–dotted line shows logarithmic creep, $\dot{\gamma}(t) \propto 1/t$. Results are for the gel with $\phi = 0.3$, $U_{\rm dep}(2R) = -5.7k_{\rm B}T$ and $\xi^* = 0.09$. The gel has been shear rejuvenated with $\gamma_0 = 1000\%$ and $\omega = 10$ rad s^{-1} and aged for the duration of 1000 s before the stress is applied.

gel deformation during creep measurements. Based on GFVT [36], increasing depletant concentration enhances the interparticle attraction strength and reduces the attraction range due to increase of osmotic pressure. Both increasing attraction strength and reducing range of attraction enhance the attractive forces and hence reduce particle mobility [57]. Moreover, increasing depletant concentration above the gelation point leads to formation of gels with more homogenous structures [5, 57] and enhanced elasticity [5].

Here, we present the creep response for the gel with lower depletant concentration and hence weaker attraction strength of $U_{\rm dep}(2R) = -5.7k_{\rm B}T$ and larger attraction range of $\xi^* = 0.09$. The gel has been shear rejuvenated at the strain amplitude of $\gamma = 1000\%$ with the frequency $\omega = 10$ rad s^{-1} and then aged for the duration of 1000 s before shear stress is applied. Results of creep measurements for this gel are shown in figure 4. Similar to the stronger gel ($U_{\rm dep}(2R) = -12.7k_{\rm B}T, \xi^* \simeq 0.06$) presented in figure 1, here the weaker gel also shows three regimes of creeping for $\sigma < 0.5$ Pa, resolidification for 0.5 Pa $< \sigma <$ 0.9 Pa and viscous flow for $\sigma > 0.8$ Pa. The weaker gel shows a smaller value of the stress threshold for the long-time viscous flow ($\sigma_{\rm f} = 0.9$ Pa) compared to the stronger gel of $-12.7k_{\rm B}T$ ($\sigma_{\rm f} = 1.6$ Pa). As mentioned above, in the stronger gel, due to both enhanced attraction strength and reduced range of attraction, attractive forces are stronger and hence bond breaking and flow require larger forces eventually resulting to higher yield stress.

The stark contrast between weaker and stronger gel is detected however in the resolidification regime. In the case of the stronger gel, resolidification takes place gradually (see figure 1). In contrast, the weaker gel shows an abrupt resolidification (figure 4). Although the microscopic origin of such abrupt resolidification needs more complementary techniques such as rheo-confocal experiments and computer simulations, here, we provide evidences that such abrupt resolidification may originate from the enhanced structural heterogeneity in the weaker gel. To support this idea, in section 3.1.3, we will examine the role of preshear history which also has a profound impact on the structural heterogeneity.

In figure 5, we compare the creep response of the weak and strong gels at three stress regimes, namely below the yield stress, in the resolidification and viscous flow regimes. Such a comparison provides a more detailed picture about the influence of bond strength and length (depletant concentration) on the gel deformation during creep measurements.

For $\sigma < \sigma_y$, the stronger gel exhibits smaller values of creep compliance compared to the weaker one. As mentioned earlier, in the gel with higher concentration of depletants attractive forces are stronger and hence particle mobility is less. Such reduced particle mobility is expected to result in a lower values of $J(t)$ (see equation (2)). Moreover, lower values of $J(t)$ for stronger gel means enhanced elasticity compared to the weaker gel since $G^* \sim 1/J(t)$. This is in agreement with the linear viscoelastic measurements shown in figure S2.

When the shear stress is increased to 0.7 Pa, the weaker gel yields and flows after a delay time although it eventually resolidifies abruptly at long-times. In contrast, the stronger gel shows longer time creeping behavior without yielding. The initial ballistic increase of $J(t)$ takes place at shorter times for the weaker gel in which thermal fluctuations are more active. Similarly, as shown in figure 3, the younger gel in which particles are more mobile also yields faster. Hence, one can conclude that Brownian motions assist particles to escape bonds and hence facilitate yielding as discussed above.

In the viscous flow regime, the weaker gel shows larger values of both creep compliance and shear rate. Higher flow rates (at a constant stress) in the weaker gel originate, microscopically, from a faster shear-induced particle diffusion (see equation (2)).

3.1.3. Effect of the preshear. We now further examine the effect of preshear history on the yielding behavior of colloidal gels during creep experiments. Colloidal gels due to their nonequilibrium nature are very sensitive to preparation history. It has been shown that shear flow largely affects their structure and consequently their mechanical properties [16, 17]. In our previous work, we have demonstrated that oscillatory preshear is a more efficient way to create gels with larger structural

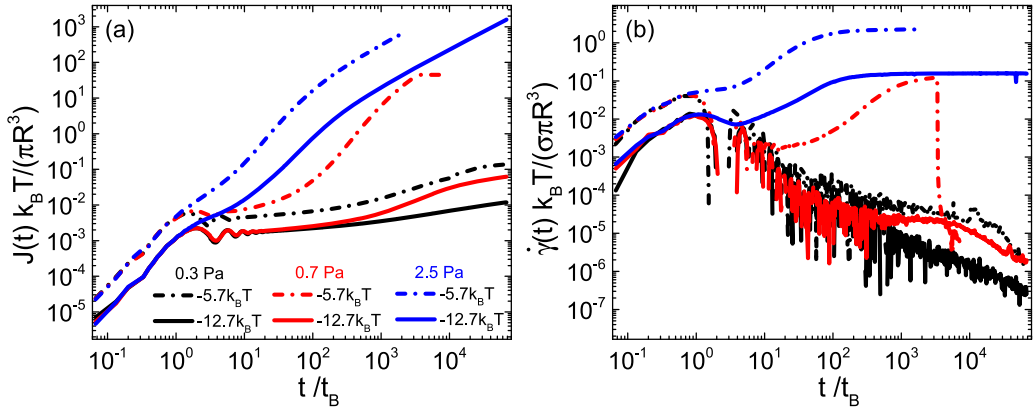

Figure 5. (a) Creep compliance and (b) the shear rate as a function of time at different applied shear stresses as shown in the legend for two different attraction strengths of $U_{\rm dep}(2R) = -5.7k_{\rm B}T$ (dashed–dotted lines) and $-12.7k_{\rm B}T$ (solid lines). The gel has been shear rejuvenated with $\gamma_0 = 1000\%$ and $\omega = 10$ rad s^{-1} and aged for the duration of 1000 s before the stress is applied.

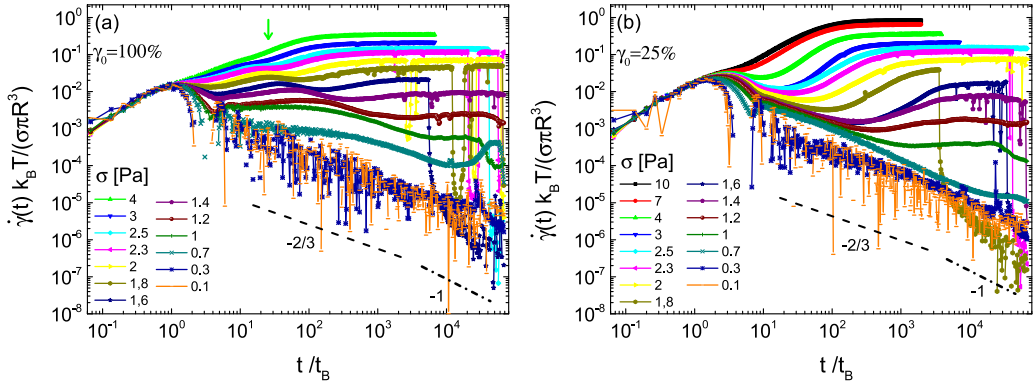

Figure 6. The shear rate as a function of time at different applied shear stresses as shown in the legend for the gel presheared with $\omega = 10$ rad s^{-1} at the strain amplitudes of $\gamma_0 =$ (a) 100% and (b) 25%. Dashed lines represent Andrade creep law, $\dot{\gamma}(t) \propto t^{-2/3}$ and dashed–dotted lines show logarithmic creep, $\dot{\gamma}(t) \propto 1/t$. The vertical arrow in (a) shows the indicative delay yield time (for $\sigma = 4$ Pa) taken from the second superlinear growth of bulk deformation. Results are for the gel with $\phi = 0.3$, $U_{\rm dep}(2R) = -12.7k_{\rm B}T$ and $\xi^* = 0.058$. After the preshear, the gel has been aged for the duration of 1000 s before the stress is applied.

heterogeneity and hence reduced elasticity compared to steady shear flow [17]. Therefore, in the present study, we chose oscillatory shear flow in order to create gels with different levels of structural heterogeneity and hence different elasticity.

In order to erase any shear history effects, the gel was fully shear rejuvenated at strain amplitude of $\gamma_0 = 1000\%$ with the frequency $\omega = 10$ rad s^{-1}. Then, the gel was subjected to an oscillatory shear flow with the same frequency but strain amplitudes of 100% and 25%. After reaching steady oscillatory shear flow, shear was stopped and the gel was allowed to age for the duration of 1000 s. Dynamic frequency sweep measurements in the linear viscoelastic regime show a solid-like response manifested by larger values of storage modulus G' compared to loss modulus G'' over the entire range of probed frequency (see figure S3). Moreover, a decrease in the strain amplitude of the preshear leads to formation of gels with weaker elasticity (figure S3). This is due to an enhanced structural heterogeneity which reduces the number of bonds that connect the clusters together [17].

Now, we turn our attention to the creep response of the gel prepared at different preshear strain amplitudes. The results for the gel presheared with $\gamma_0 = 1000\%$ has already been shown in figure 1. In figures 6(a) and (b), we present the creep experiments for the gel presheared at strain amplitudes of $\gamma_0 = 100\%$ and 25%, respectively. In this case, similar to the gel presheared at $\gamma_0 = 1000\%$, one can identify three regimes of (i) below yield stress (ii) resolidification and (iii) viscous flow. However, the marked contrast with the more *homogenous gel* prepared by preshearing at large strain of $\gamma_0 = 1000\%$ is detected in the resolidification regime. As shown in figure 1, the gel presheared at $\gamma_0 = 1000\%$ resolidifies gradually whereas those presheared at $\gamma_0 = 100\%$ and 25% show a sudden resolidification after reaching a well-defined viscous flow. Moreover, in the case of the gel presheared with $\gamma_0 = 100\%$, this sudden resolidification is accompanied by successive abrupt yielding and resolidification (see $\sigma = 2.3$, 2 and 1.8 Pa in figure 6(a). For a better clarity, we have shown the results for $\sigma = 2$ and 2.3 Pa separately in figure S4.

In order to highlight the detailed differences caused by preshear during the creep measurements, we contrast the creep compliance and the shear rate for the gel presheared at

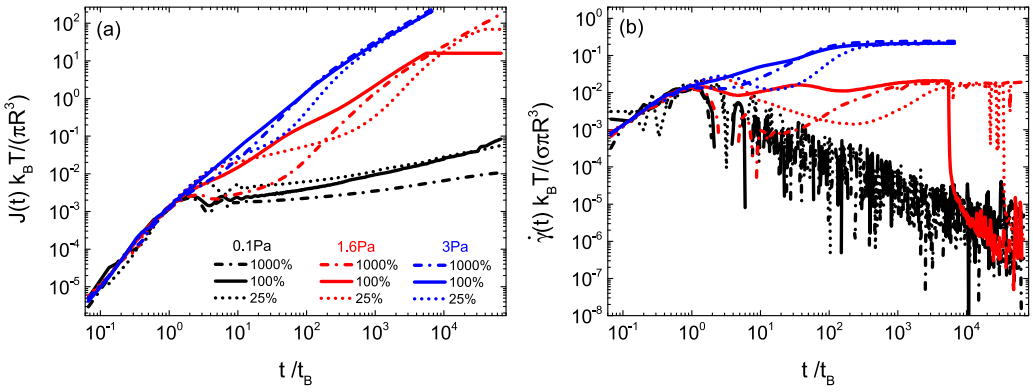

Figure 7. (a) Creep compliance and (b) the shear rate as a function of time at different applied shear stresses as shown in the legend. The gel has been presheared with $\omega = 10$ rad s^{-1} at different strain amplitudes of 1000% (dashed–dotted lines), 100% (solid lines) and $\gamma_0 = 25\%$ (dashed lines). Results are for the gel with $\phi = 0.3$, $U_{\rm dep}(2R) = -12.7 k_{\rm B}T$ and $\xi^* = 0.058$. After the preshear, the gel has been aged for the duration of 1000 s before the stress is applied.

different strain amplitudes of $\gamma_0 = 1000\%$, 100% and 25% at different regimes: (i) below the yield stress (ii) in the resolidification regime and (iii) viscous flow regime. Results of such comparison are shown in figure 7. For $\sigma < \sigma_y$, the gel presheared at larger strain amplitudes exhibits lower values of creep compliance. Microscopically, this indicates, based on equation (2), that in more homogenous gels that are created by preshearing at larger strain amplitudes, particles are less mobile. A smaller particle mobility leads to an enhanced elasticity since $G^* \sim 1/J(t)$ in agreement with linear viscoelastic measurements presented in figure S3.

For $\sigma > \sigma_y$, the time at which the superlinear increase of $J(t)$ commences, shows a non-monotonic dependence with the strain amplitude of preshear. This time is shortest for the gel presheared at the intermediate strain amplitude of 100% and longest for the gel presheared at lowest strain amplitude of 25%. In contrast, the gel presheared at the large strain amplitude of 1000% shows a time between the two.

A careful inspection of the creep compliance and shear rate in figure 7 for $\sigma = 1.6$ and 3 Pa for the gel presheared at *intermediate* strain amplitude of 100% marks an interesting feature. In this case, the transient $J(t)$ shows a two-step superlinear growth during the creep measurements. As the result, the flow rate also shows a two-step growth before reaching a constant value at long-times indicating complete yielding and flow. Such a two-step superlinear growth of $J(t)$ indicates that the gel presheared at intermediate strain amplitude of 100% yields in a two-step process. Two-step yielding is seen for all shear stresses above the yield stress (see figure 6(a)). Two-step yielding has been observed during both start-up shear flow and dynamic strain sweep measurements in colloidal gels [17, 38, 54, 58] and attractive colloidal glasses [38, 47, 59, 60] where the first yield has been associated to a short length scale bond breaking and restructuring whereas the second yield to a larger length scale breakage and restructuring of clusters (in colloidal gels) or cages (in attractive glasses). In our previous work, we have demonstrated that preshear has a strong impact on the yielding behavior of colloidal gels during start-up shear flow experiments [17]. More homogenous gels that are produced by oscillatory preshear at large strain amplitudes exhibit a nearly single step yielding process. In contrast, those gels that are prepared by preshearing at low and intermediate strain amplitudes (and equivalently lower shear rates) yield in a two-step process due to an enhanced structural heterogeneity caused during preshear. The magnitudes of the first and the second yield processes, manifested by the magnitude of the corresponding stress peaks, depend on the preshear strain amplitude. In gels that are presheared at *low* strain amplitudes, the magnitude of the first yield process is rather weak and probably that is why the gel presheared at lower strain amplitude of 25% does not show a two-step yielding during creep measurements.

The long-time creep compliance and the shear rate in the viscous flow regime (see creep results for $\sigma = 3$ Pa in figure 7) are independent of the preshear strain amplitude although the transient response towards the long-time steady state is affected by preshear. As mentioned earlier, this marks a unique shear-melted state where the structural history caused during the course of preshear has been completely erased by shear flow.

In contrast, in the resolidification regime, although initially the flow rate for all three different preshear strain amplitudes reaches the same constant value (see $\sigma = 1.6$ Pa in figure 7(b)), eventually the difference between different preshears emerges at longer-times where the more heterogenous gels produced by preshearing at lower strain amplitudes of 100% and 25%, resolidify abruptly whereas the more *homogenous gel* prepared by preshearing at large strain amplitude of $\gamma_0 = 1000\%$, does not resolidify. In this case, $\gamma_0 = 1000\%$, resolidification takes place at lower stresses (0.7 Pa $< \sigma <$ 1.6 Pa) and as shown earlier in figures 1 and 2, occurs gradually. These findings further supports the idea that the abrupt resolidification originates from enhanced structural heterogeneity. However, the mechanism by which the structural heterogeneity impacts the rate of resolidification remains to be explored. We must also note that creep results for stresses below yield stress and in the viscous flow regime are highly reproducible. In contrast, in the resolidification regime and especially for those gels presheared at low strain amplitudes of 25% and 100%, the time at which resolidification takes place is varying from test to test, suggesting

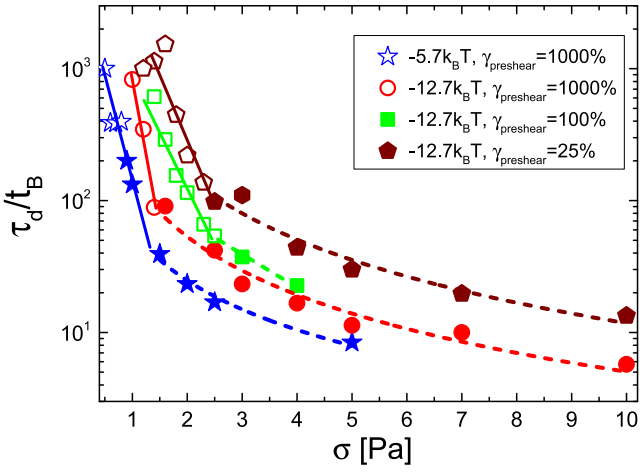

Figure 8. The delay time as a function of the applied shear stress at different attraction strengths and preshear strain amplitudes as shown in the legend. Open symbols are related to stresses where resolidification under stress takes place whereas closed symbols represent stresses at which a viscous flow is reached. The solid lines are the exponential fits and the dashed lines are power law fits to experimental data. In all cases, the gel has been aged for the duration of 1000 s before the stress is applied.

that there is a certain level of uncertainty probably introduced by internal chaotic rearrangements or to some extent external conditions.

3.1.4. The delay time. In this section, we examine variations of the delay yield time τ_d with the strength of the external load, interparticle attraction strength as well as the role played by shear rejuvenation. Here, we adopt the definition used by Sprakel *et al* [27] for the delay time defined as the required time for the derivative of the shear rate ($d\dot{\gamma}/dt$) to reach its maximum i.e. the time after which the acceleration of shear flow slows down (see indicative vertical arrows in figure 1(b)). In figure 8, we plot the delay time as a function of shear stress for the gels with two different attraction strengths of -5.7 and $-12.7k_BT$. For the stronger gel of $-12.7k_BT$, the delay time for different preshear strain amplitudes is also shown. For the gel presheared at the strain amplitude of 100%, the delay time was calculated for the second-step superlinear growth of $J(t)$ (as shown in figure 6(a) by the indicating vertical arrow). All the results are after the gel was aged for 1000 s. The delay time increases as the attraction strength is increased or the strain amplitude of preshear is reduced. Moreover, in all cases, the delay time decreases with shear stress exhibiting two distinct scaling regimes: an exponential decay for weak stresses and a power-law for stronger shear stresses with $\tau_d \sim \sigma^{-\alpha}$ with α found to be 1.2–1.6. This behavior is consistent with findings by BD simulation on similar, yet lower volume fraction, colloidal gels [25] while previous experiments with a variety of attractive colloidal gels, including depletion systems at lower ϕ, suggest a double exponential decrease [27]. Such two distinct scaling regimes of the delay time has been explained based on a bond-rupture model [27]. In the strong-stress regime, the rate of bond breakage is larger than bond reformation. Therefore, the failure of the entire network takes place approximately at the same rate as the breakage of single bonds which based on the single-bond-rupture model is predicted to be an exponential function of stress although in our case it follows a power-law decay. On the other hand, at the limit of weak stress regime, the rate of bond breakage is smaller than the bond reformation and hence, yielding requires a simultaneous dissociation of all bonds within a cross section of a network strand. This process is also an exponential function of the applied load, but with a different characteristic stress [27].

The most striking observation in figure 8 is that the resolidification takes place in the 'weak-stress regime' where a net bond formation occurs under stress consistent with findings from BD simulations [25]. In the case of the stronger gel, the transition from weak-stress regime (net bond gain) to strong-stress regime (net bond loss) coincides with the transition from resolidification to viscous flow regime. For the weaker gel, however, resolidification takes place well inside the weak-stress regime. Moreover, as it is clearly demonstrated in figure 8, the suppression of Brownian motion by increasing attraction strength and particle localization leads to an increase of the delay time for yielding, suggesting that thermal fluctuations act in cooperation with shear to promote yielding via bond rearrangement and breaking. This is in line with earlier strain controlled experiments [5, 47, 55, 56] and the BD simulations [25] discussed above.

3.2. Stress vs strain controlled shear experiments

As a final point, we compare the stress versus strain controlled experiments under *steady state* shear flow conditions. In strain controlled experiments a constant shear rate is imposed and the evolution of the stress with time is probed. In this study, the transient evolution of the stress is not the subject of interest and hence only the steady state condition is considered. In figure 9, we present the steady state values of shear stress as a function of the applied shear rate (flow curve) for the weak gel of $-5.7k_BT$. The flow curve exhibits a typical response for colloidal gels. A well-developed yield stress plateau emerges at low shear rates indicating the dynamic yield stress. As mentioned in section 2, the presence of a single yield stress plateau is the rheological fingerprint of no wall-slip conditions. For shear rates slightly above the yield stress plateau, the stress exhibits a sublinear growth with shear rate which marks shear-thinning response. Microscopic imaging in this regime indicates formation of heterogenous structures under shear flow in which heterogeneity is progressively reduced as shear flow is enhanced [16, 39]. However, at very high shear rates (well above $Pe_{dep} = 1$), the gel tends to behave as a simple Newtonian fluid in which the stress increases linearly with the imposed shear rate as the result of the full break-down of the gel structure [16, 39]. In figure 9, we also show results for stress controlled (creep) experiments when a steady state shear flow is reached (blue star symbols). Note that in creep experiments, the steady state condition is achieved only in the viscous flow regime. In figure 9, we also show the value of yield stress taken from creep measurements (horizontal dashed line). As mentioned, in creep experiments the yield

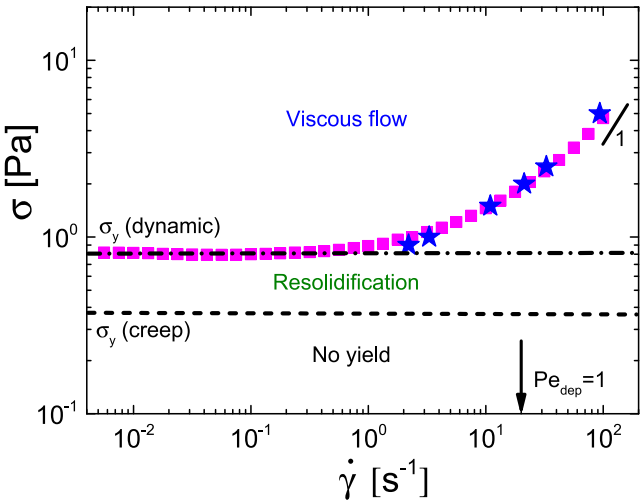

Figure 9. Steady state shear stress as a function of the applied shear rate (pink squares). Blue star symbols are the steady state values taken from creep experiments. The horizontal dashed–dotted line shows the dynamic yield stress (the stress plateau) whereas dashed line represents the yield stress measured from creep experiments. The vertical arrow represents $Pe_{\rm dep} = 1$. Results are for the gel with $\phi = 0.3$, $U_{\rm dep}(2R) = -5.7k_{\rm B}T$ and $\xi^* = 0.09$.

stress is defined as the stress below which the creep compliance becomes independent of the applied stress. As shown in figure 9, the yield stress taken from creep measurement is well below the dynamic yield stress (horizontal dashed–dotted line) taken from the stress plateau in strain controlled experiments.

A comparison between stress and strain controlled experiments indicates that the yield stress plateau is the stress which distinguishes viscous flow regime from resolidification and no yield regimes. If the applied stress is larger than the dynamic yield stress, then the gel will ultimately yield and flow (blue star symbols). In this case, both strain and stress controlled experiments result into the same steady state conditions. This demonstrates that in the viscous flow regime, the path towards steady state is not important as also observed in figures 3 and 7. If the imposed stress is below the dynamic yield stress and above the creep yield stress, the gel temporarily flow but eventually resolidifies. In contrast, for stresses below the creep yield stress, the gel will never yield.

4. Conclusions

The bulk deformation in a frustrated, out-of-equilibrium, particle gel have been investigated during creep measurements. The model system is comprised of hard-sphere colloidal particles with a volume fraction of $\phi = 0.3$ where short-ranged attractions are introduced between particles by adding nonadsorbing linear polymer chains. The influence of the applied shear stress, gel age, interparticle attraction strength and the preshear history on the bulk deformation and yielding of the gel during creep measurements have been explored.

The creep yield stress is defined as the stress below which the creep compliance becomes stress-independent whereas the dynamic yield stress is defined as the low shear rate stress plateau measured by a decreasing shear rate (flow curve). We find that the creep yield stress is well below the dynamic yield stress. The gel exhibits three well-defined response regimes: (i) when the applied stress is below the creep yield stress, the gel undergoes a weak sublinear deformation in which the shear rate $\dot{\gamma}$ continues to decay indefinitely with time. The long-time preyield creep response follows $\dot{\gamma}(t) \propto 1/t$ similar to crystalline and amorphous solids.

When shear stress is increased above the creep yield stress, initially, the gel deformation follows the sublinear growth. However, when deformation reaches the order of the attraction range, it turns into a ballistic growth which signals yielding of the gel. As stress is enhanced, the transition from sublinear to superlinear growth takes place at shorter times. Moreover, in younger gels or gels with reduced interparticle attractions in which the particle mobility is enhanced, this transition occurs at shorter times indicating a faster yielding. This suggests that Brownian motions assist the particles to escape their bonds and hence facilitate yielding. Microscopically, such superlinear growth of bulk deformation is associated to ballistic motions of particles when they leave their attractive bonds. After the superlinear growth of deformation, two distinct responses emerge: (ii) in the presence of strong stresses (above the dynamic yield stress), the gel deforms linearly with time which indicates the development of a steady state viscous flow and hence a complete yielding. In contrary, (iii) under weak shear stresses (between creep and dynamic yield stresses), the gel starts to resolidify under stress. This is manifested by a transition from a superlinear to a sublinear growth of bulk deformation. The analysis of the delay yield time indicates that resolidification takes place in the weak stress regime in which a net bond formation and hence gel coarsening under stress occurs.

The examination of the gel age, interparticle attraction strength as well as preshear history indicates that the rate at which resolidification takes place depends on the structural heterogeneity. In gels with relatively homogenous structures, resolidification takes place gradually whereas in gels with more heterogenous structures resolidification occurs abruptly. Finally, a two-step yielding process is detected for heterogenous gels that are produced by oscillatory preshear at the intermediate strain amplitude. This is manifested by a two-step superlinear growth of bulk deformation during creep experiments. These findings demonstrate the rich nonlinear flow response of colloidal gels under constant stress that are due to microscopic interplay of shear induced bond formation and breakage or restructuring with Brownian motion; all the above affected by pre-existing structures formed during a specific shear flow history.

Acknowledgments

Authors acknowledge EU funding through the innovation program ‘EUSMI’ (Grant agreement No. 731019).

Data availability statement

All data that support the findings of this study are included within the article (and any supplementary files).

ORCID iDs

George Petekidis https://orcid.org/0000-0001-5418-697X

References

[1] Mewis J and Wagner N J 2012 *Colloidal Suspension Rheology* (Cambridge: Cambridge University Press)
[2] Petekidis G and Wagner N J 2021 Rheology of colloidal glasses and gels *Theory and Applications of Colloidal Suspension Rheology* ed J Mewis and N J Wagner (Cambridge: Cambridge University Press)
[3] Chen Y-L and Schweizer K S 2004 *J. Chem. Phys.* **120** 7212–22
[4] Shah S A, Chen Y-L, Schweizer K S and Zukoski C F 2003 *J. Chem. Phys.* **119** 8747–60
[5] Laurati M, Petekidis G, Koumakis N, Cardinaux F, Schofield A B, Brader J M, Fuchs M and Egelhaaf S U 2009 *J. Chem. Phys.* **130** 134907
[6] Lu P J, Zaccarelli E, Ciulla F, Schofield A B, Sciortino F and Weitz D A 2008 *Nature* **453** 499–503
[7] Pham K N *et al* 2002 *Science* **296** 104–6
[8] Eberle A P R, Castañeda-Priego R, Kim J M and Wagner N J 2012 *Langmuir* **28** 1866–78
[9] Joshi Y M and Petekidis G 2018 *Rheol. Acta* **57** 521–49
[10] Mewis J 1979 *J. Non-Newton. Fluid Mech.* **6** 1–20
[11] Mewis J and Wagner N J 2009 *Adv. Colloid Interface Sci.* **147–148** 214–27
[12] Koumakis N, Laurati M, Jacob A R, Mutch K J, Abdellali A, Schofield A B, Egelhaaf S U, Brady J F and Petekidis G 2016 *J. Rheol.* **60** 603–23
[13] Sentjabrskaja T, Chaudhuri P, Hermes M, Poon W, Horbach J, Egelhaaf S and Laurati M 2015 *Sci. Rep.* **5** 11884
[14] Jacob A R, Moghimi E and Petekidis G 2019 *Phys. Fluids* **31** 087103
[15] Choi J and Rogers S A 2020 *Rheol. Acta* **59** 921–34
[16] Koumakis N, Moghimi E, Besseling R, Poon W C K, Brady J F and Petekidis G 2015 *Soft Matter* **11** 4640–8
[17] Moghimi E, Jacob A R, Koumakis N and Petekidis G 2017 *Soft Matter* **13** 2371–83
[18] Poon W C K and Haw M D 1997 *Adv. Colloid Interface Sci.* **73** 71–126
[19] Kim J M, Fang J, Eberle A P, Castañeda-Priego R and Wagner N J 2013 *Phys. Rev. Lett.* **110** 208302
[20] Ballesta P, Koumakis N, Besseling R, Poon W C K and Petekidis G 2013 *Soft Matter* **9** 3237–45
[21] Divoux T, Fardin M A, Manneville S and Lerouge S 2016 *Annu. Rev. Fluid Mech.* **48** 81–103
[22] Gibaud T, Frelat D and Manneville S 2010 *Soft Matter* **6** 3482–8
[23] Zia R N, Landrum B J and Russel W B 2014 *J. Rheol.* **58** 1121–57
[24] Johnson L C, Zia R N, Moghimi E and Petekidis G 2019 *J. Rheol.* **63** 583–608
[25] Landrum B J, Russel W B and Zia R N 2016 *J. Rheol.* **60** 783–807
[26] Christopoulou C, Petekidis G, Erwin B, Cloitre M and Vlassopoulos D 2009 *Philos. Trans. R. Soc.* A **367** 5051–71
[27] Sprakel J, Lindström S B, Kodger T E and Weitz D A 2011 *Phys. Rev. Lett.* **106** 248303
[28] Lindström S B, Kodger T E, Sprakel J and Weitz D A 2012 *Soft Matter* **8** 3657–64
[29] Grenard V, Divoux T, Taberlet N and Manneville S 2014 *Soft Matter* **10** 1555–71
[30] Ballesta P and Petekidis G 2016 *Phys. Rev.* E **93** 042613
[31] Siebenbürger M, Ballauff M and Voigtmann T 2012 *Phys. Rev. Lett.* **108** 255701
[32] Gopalakrishnan V and Zukoski C F 2007 *J. Rheol.* **51** 623–44
[33] Calzolari D C E, Bischofberger I, Nazzani F and Trappe V 2017 *J. Rheol.* **61** 817–31
[34] Leocmach M, Perge C, Divoux T and Manneville S 2014 *Phys. Rev. Lett.* **113** 038303
[35] Brenner T, Matsukawa S, Nishinari K and Johannsson R 2013 *J. Non-Newton. Fluid Mech.* **196** 1–7
[36] Fleer G J and Tuinier R 2007 *Phys. Rev.* E **76** 041802
[37] Asakura S and Oosawa F 1954 *J. Chem. Phys.* **22** 1255–6
[38] Koumakis N and Petekidis G 2011 *Soft Matter* **7** 2456–70
[39] Moghimi E, Jacob A R and Petekidis G 2017 *Soft Matter* **13** 7824–33
[40] Squires T M and Mason T G 2010 *Annu. Rev. Fluid Mech.* **42** 413–38
[41] Xu J, Viasnoff V and Wirtz D 1998 *Rheol. Acta* **37** 387–98
[42] Mason T G 2000 *Rheol. Acta* **39** 371–8
[43] Vyas B M, Orpe A V, Kaushal M and Joshi Y M 2016 *Soft Matter* **12** 8167–76
[44] Levine A J and Lubensky T 2001 *Phys. Rev.* E **63** 041510
[45] Sierou A and Brady J F 2001 *J. Fluid Mech.* **448** 115–46
[46] Baravian C, Benbelkacem G and Caton F 2007 *Rheol. Acta* **46** 577–81
[47] Moghimi E and Petekidis G 2020 *J. Rheol.* **64** 1209–25
[48] Moghimi E, Vermant J and Petekidis G 2019 *J. Rheol.* **63** 533–46
[49] Andrade E N D C 1910 *Proc. R. Soc. Lond.* A **84** 1–12
[50] Divoux T, Barentin C and Manneville S 2011 *Soft Matter* **7** 8409–18
[51] Phillips P 1905 *The London, Edinburgh, and Dublin Philosophical Magazine and Journal of Science* **9** 513–31
[52] Nguyen V B, Darnige T, Bruand A and Clement E 2011 *Phys. Rev. Lett.* **107** 138303
[53] Johnson L C, Landrum B J and Zia R N 2018 *Soft Matter* **14** 5048–68
[54] Laurati M, Egelhaaf S U and Petekidis G 2011 *J. Rheol.* **55** 673–706
[55] Koumakis N, Brady J and Petekidis G 2013 *Phys. Rev. Lett.* **110** 178301
[56] Koumakis N, Laurati M, Egelhaaf S, Brady J and Petekidis G 2012 *Phys. Rev. Lett.* **108** 098303
[57] Dibble C J, Kogan M and Solomon M J 2006 *Phys. Rev.* E **74** 041403
[58] Chan H K and Mohraz A 2012 *Phys. Rev.* E **85** 041403
[59] Pham K N, Petekidis G, Vlassopoulos D, Egelhaaf S U, Pusey P N and Poon W C K 2006 *Europhys. Lett.* **75** 624
[60] Pham K N, Petekidis G, Vlassopoulos D, Egelhaaf S U, Poon W C K and Pusey P N 2008 *J. Rheol.* **52** 649–76